International Journal of Engineering Trends and Technology
ISSN: 2231–5381 / https://doi.org/10.14445/22315381/IJETT-V73I9P105
Volume 73 Issue 9, 48-53, September 2025

Original Article

Measurement of Water Droplet Diameter Using Experiment, Theory and High-Speed Visualization Technique

D. Sarravanan[1], S. Illias[1*], S. Hussain[1], M. S. Mohamad[1], M. H. Ani[2]

[1]*Faculty of Mechanical Engineering & Technology, Universiti Malaysia Perlis, Pauh Putra Campus, Perlis, Malaysia.*
[2]*Department of Manufacturing and Materials, Kulliyah of Engineering, International Islamic University Malaysia, Kuala Lumpur, Malaysia.*

[1]*Corresponding Author : suhaimi@unimap.edu.my*

Received: 15 April 2025 Revised: 12 August 2025 Accepted: 30 August 2025 Published: 30 September 2025

Abstract - *Before starting any experimental work regarding droplet impact experiments, it is very important to verify and confirm the droplet size and diameter. The main reason behind this would be to ensure that every single droplet is almost of the same size before any scientific analysis is carried out. Therefore, the aim of this study is to perform a single water droplet diameter measurement through experimental work, theoretical calculation and high-speed digital imaging technique. In the experimental work, distilled water was used as a test liquid. A digital microscope was used to measure the inner and outer sizes of the droplet dispenser nozzle. The water drop test was performed up to 1000 times (200x5). The average reading of a single droplet weight was measured. The droplet diameter was also calculated using a theoretical calculation. On top of that, the droplet diameter was also measured using a high-speed video camera. From the overall result, it was found that the droplet diameter calculated using theoretical calculation and the one measured using high-speed video camera imaging closely agreed with each other.*

Keywords - *Droplet diameter, Nozzle size, Experimental measurement, Theoretical calculation, High-speed video camera.*

1. Introduction

The droplet impact experiment is an interesting topic of research in boiling heat transfer [1]. Topics of research that are regularly conducted by researchers are nucleation [2], transition [3-5], and film boiling [6-8]. These three (3) areas are the important modes in the research area of boiling heat transfer. In general, experimental work is conducted with the use of high-speed video cameras to view sequential images of droplets during impact on a test surface. The sequential images obtained during the experimental work can be used to study the evaporation characteristics, droplet size, droplet spreading [9, 10], and bouncing [11, 12] of the droplet. Furthermore, the research findings are broadly used in many engineering applications such as spray cooling [13, 14], boilers [15], fuel combustion [16], inkjet printing technology [17, 18], and coating technology [19, 20]. Moreover, the insight into droplet interfacial dynamics is essential in controlling parameters like wettability [21], impact speed, and surface temperature. Apart from that, research on Leidenfrost [22-25] is also very important in the field of heat transfer, which greatly influences the heat transfer performance [26]. In boiling experiments, preliminary tests on droplet size must be carried out first to determine the accuracy of the final results of the experiment. If the droplet size used is not uniform, it will have a very significant impact on the final results. The novelty of this research is the use of three (3) different methods in determining the droplet size. After conducting two (2) different tests (i.e., theoretical calculation and experiment), the third test, which used a high-speed video camera, was used to determine the droplet size. Based on the observations and literature review, no other researchers have used three different approaches in determining droplet size before the actual test was carried out. Most researchers only carry out size tests using a high-speed video camera to determine droplet size. This is done via a comparison technique whereby the size of the droplet falling onto a surface is compared to the actual size of a screw or other objects. However, for this paper, the final results obtained for each droplet size would be very convincing because these three (3) different techniques had been used to determine the droplet size.

2. Experimental Apparatus and Procedure

The schematic diagram of the experimental setup of the drop test is shown in Figure 1. For the current experiment, distilled water was used as the test liquid. The experimental setup consisted of a droplet dispenser, beaker, retort stand, and digital weight (MH-100 pocket scale). The droplet dispenser was slowly and gently pressed to ensure the droplet fell slowly into the glass beaker.

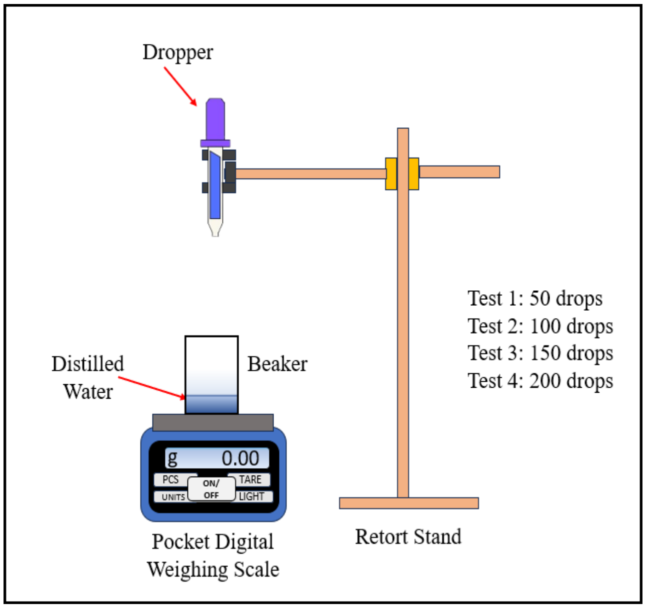

Fig. 1 Schematic diagram of the drop test set-up

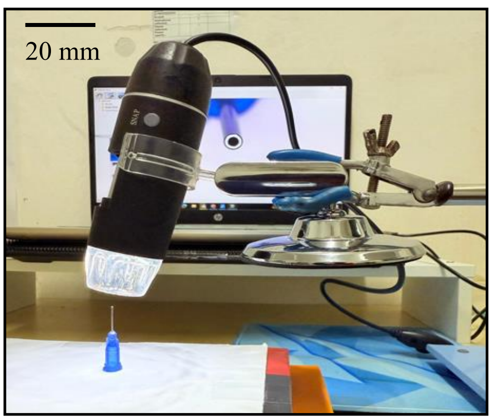

(a) Digital microscope

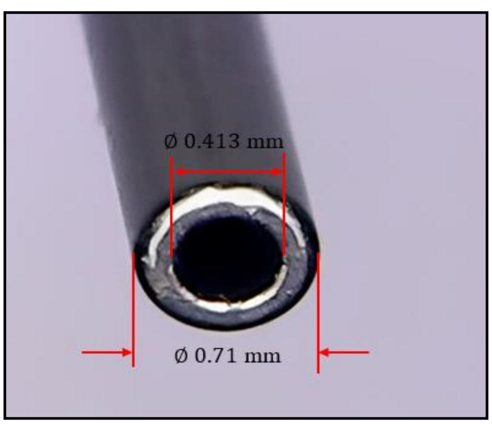

(b) Close-up image

Fig. 2 Digital microscope and measurement technique of the outer and inner nozzle dispenser

Meanwhile, Figure 2 shows the digital microscope setup and a close-up image of the nozzle dispenser. The digital microscope was connected to a laptop for digital visual analysis. From the visual observation of Figure 2(b), the inner nozzle size was approximately 0.413 mm. Meanwhile, Figure 3 shows the actual image of the outer nozzle measured using the Quick-Mini Thickness Gage (Mitutoyo PK-0505). From the digital measurement, the outer diameter of the nozzle was approximately 0.71 mm. During the experimental work, a high-speed video camera (i-SPEED 221) was used to record the images of the droplet as it fell (Figure 4). The falling droplet was recorded at 5,000 frames per second (fps).

Table 1. Experimental conditions

Type of liquid	Distilled Water
Surface tension of distilled water, σ (N/m)	0.0728
Density of distilled water, ρ_{liq} (kg/m^3)	1000
Gravity, g (m/s^2)	9.81
Boiling point of distilled water (°C)	100
Inner nozzle size diameter (mm)	0.413
Outer nozzle size diameter (mm)	0.710

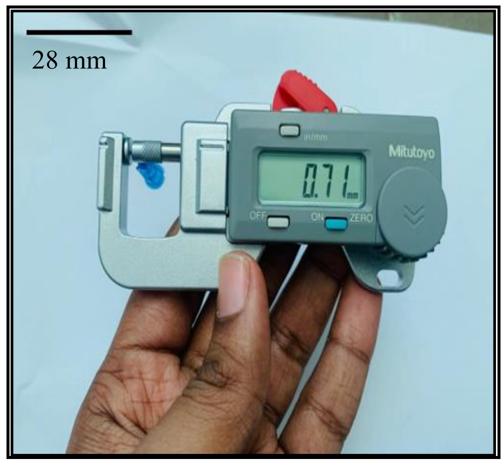

Fig. 3 Quick-mini thickness gage (Mitutoyo PK-0505)

Fig. 4 High-speed video camera set-up for digital imaging measurements

As shown in Figure 5, the Photron Fastcam Viewer (Ver. 3680 (x64)) software for high-speed digital imaging analysis was used to measure the droplet diameter. Table 1 shows the experimental conditions for the experimental work. Subsequently, Equations (1) and (2) [27] were used to calculate the droplet size experimentally and theoretically. The percentage difference was calculated using Equation (3).

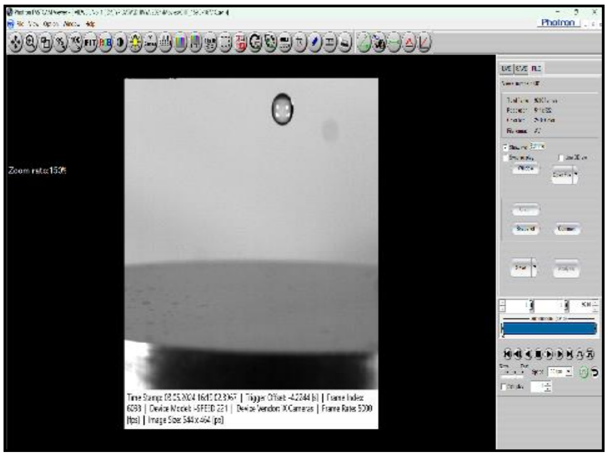

Fig. 5 Photron Fastcam Viewer (high-speed imaging software)

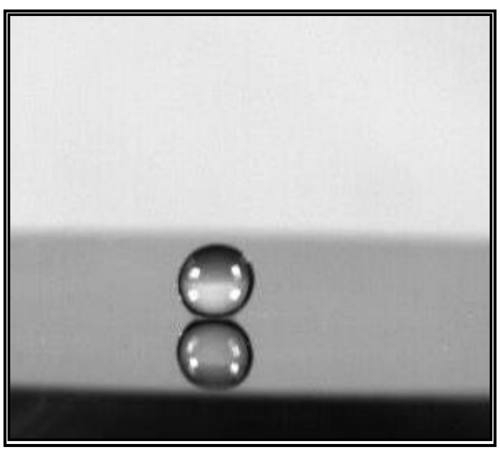
Fig. 6 Close-up image of the water droplet diameter (2.625 mm)

$$V = (4/3) \cdot \pi r^3 \quad (1)$$

$$d = (6\sigma d_{needle}/\rho_{liquid}\,(g))^{1/3} \quad (2)$$

$$\text{Percentage difference (\%)} = |\,(E_d - T_d) / (T_d)\,| \times 100\% \quad (3)$$

3. Results and Discussion

Table 2 illustrates the data collected during the drop test experiment. The experiments were repeated 5 times to enhance the accuracy of the results. To determine a single droplets average volume and weight, the drop test was performed for every 50 drops up to 200 drops. Table 2 clearly shows that a total of 1,000 drops were performed before determining the average value. Table 2 shows that the average value for single droplet diameter was around 2.9082 mm. At the beginning of test 1 (50 drops), the weight of the droplet was about 0.66 g, followed by 0.64 g for tests 2 and 3, and 0.62 and 0.65 g for tests 4 and 5, respectively. The weights of the droplets seemed to increase to about 1.27 g for tests 1 and 2 when the number of drops was increased to 100 drops. For the 150 drop, tests 1, 2 and 3, the data recorded were 1.93, 1.91, and 1.95 g, respectively. Finally, at 200 drops, tests 1-5 weight outputs represented an increase of approximately 2.58, 2.55, 2.60, 2.58, and 2.59 g, respectively.

Table 2 also indicates that the average data calculated from the drop tests were approximately 0.642 g (50 drops), 1.290 g (100 drops), 1.932 g (150 drops), and 2.580 g (200 drops). From the overall results of tests 1-5, the average mass per drop was approximately 0.01288 g. The value obtained in Equation (2), which is a theoretical calculation, was about ~ 2.637 mm. The surface tension of the water droplet, inner nozzle size diameter, density of the liquid, and gravity were used in the calculations based on Equation (2). Experimental parameters and other information are presented in Table 1 for easy understanding. A high-speed video camera was used to capture the actual size of the droplet. By using a small screw as a reference, the size of the droplet that falls from the dispenser could be measured with a digital ruler.

Table 2. Overall result from the drop test

No of Drops	Mass of Drops (gram)					Average (gram)	Average Mass per Drop (gram)	Equation (1) (mm)
	Test 1	Test 2	Test 3	Test 4	Test 5			
50	0.66	0.64	0.64	0.62	0.65	0.642	0.01284	2.9052
100	1.27	1.27	1.30	1.28	1.33	1.290	0.01290	2.9097
150	1.93	1.91	1.95	1.92	1.95	1.932	0.01288	2.9082
200	2.58	2.55	2.60	2.58	2.59	2.580	0.01290	2.9097
Average							0.01288	2.9082

The close-up image of the fallen droplet can be seen in Figure 6 as a reference. From the visual and digital analysis, the water droplet diameter was approximately 2.625 mm. Figures 7 (a)-(d) show the overall experimental results. The average values for droplet weight for 50, 100, 150, and 200 drops were 0.642, 1.290, 1.932, and 2.580 g, respectively. Figure 8 shows the average value for all the experiments. From Figure 8, it was observed that the calculated droplet diameter was approximately 2.9052, 2.9097, 2.9082, and 2.9097 mm for 50, 100, 150, and 200 drops, respectively. Meanwhile, Figure 9 shows the comparison between Equations (1) and (2) and high-speed video camera observation results. Overall data from the experimental work were tabulated in Table 2.

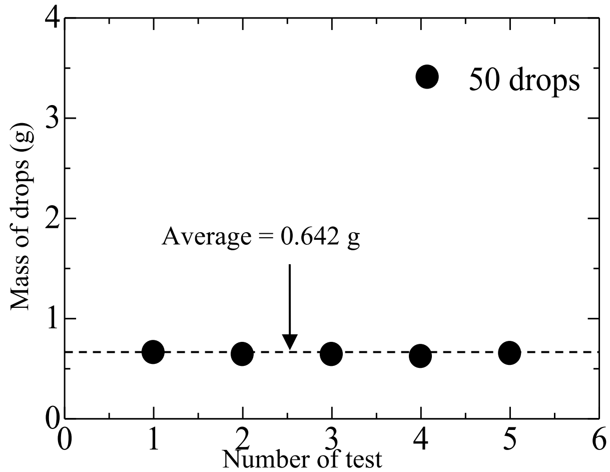

(a)

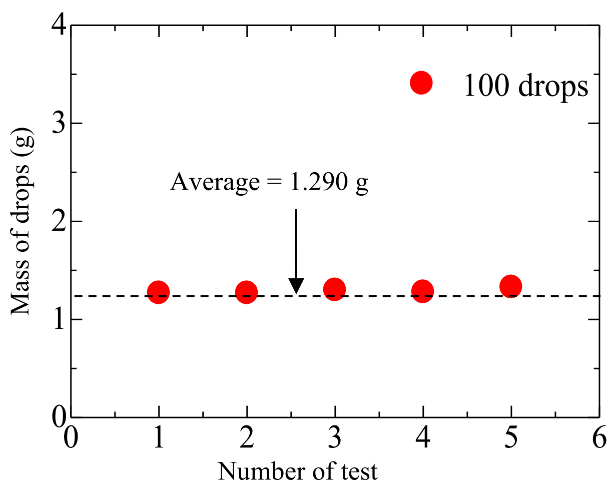

(b)

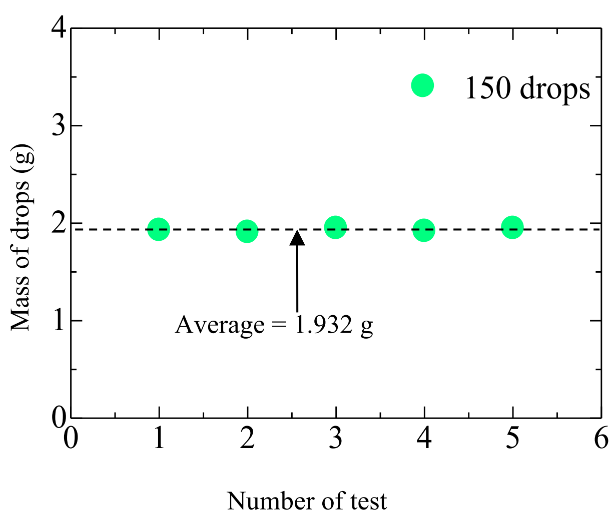

(c)

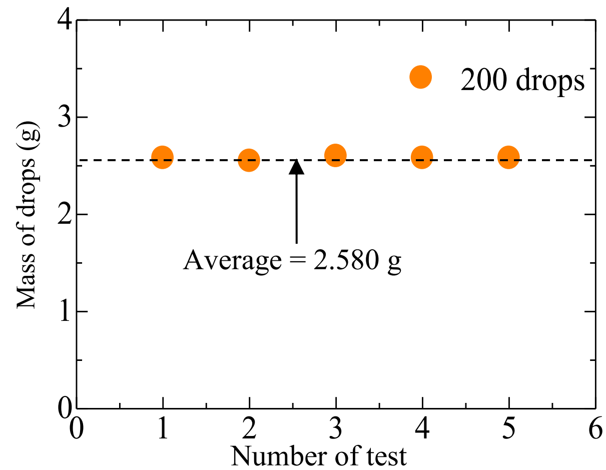

(d)

Fig. 7 Experimental result for (a) 50 drops, (b) 100 drops, (c) 150 drops, and (d) 200 drops.

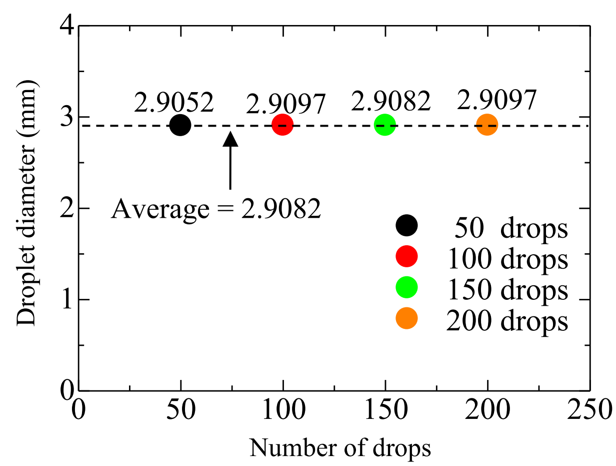

Fig. 8 Average reading for the overall experiment

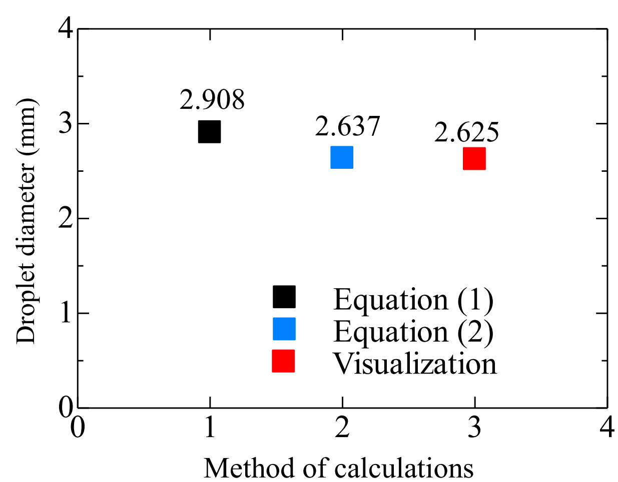

Fig. 9 Comparison result between Equations (1) and (2) and a high-speed video camera

Table 3. Comparison result between Equations (1) and (2) and a high-speed video camera

Formula	Equation (1) (mm)	Equation (2) (mm)	High-speed video camera (mm)	Percentage difference Equation (3) (%)
Droplet diameter	2.908	2.637	2.625	0.455

Table 3 compares Equations (1) and (2) with the high-speed video camera. From the overall results, it can be concluded that the final value of the droplet diameter agrees closely with the theoretical calculation, with a percentage difference of only 0.455 %.

4. Conclusion

The experimental works were conducted to investigate the diameter of the water droplet. The main interest was to compare three (3) different methods in determining the droplet diameter.

From the experiments, several conclusions can be made based on the analyses of the data collected, as well as the observations made from the high-speed imaging recorded.

The outcomes of this study are listed below:

(1) All three methods bore almost similar diameter values, with the percentage difference between the diameters measured using high-speed imaging and theory being only 0.455 %.

(2) The droplet diameter was calculated using a theoretical calculation, and the one measured using high-speed video camera imaging closely agreed with each other.

Acknowledgement

The author would like to acknowledge the Fundamental Research Grant Scheme (FRGS) support under a grant number of FRGS/1/2024/TK10/UNIMAP/02/12 from the Ministry of Higher Education Malaysia. The author would also like to thank the Faculty of Mechanical Engineering & Technology, Universiti Malaysia Perlis (UniMAP), Malaysia, for the support during the experimental work of this project.

Contributions of Authors

The authors confirm the equal contribution in each part of this work. All authors reviewed and approved the final version of this work.

References

[1] Abdoulaye Coulibaly et al., "Bubble Coalescence at Constant Wall Temperatures During Subcooled Nucleate Pool Boiling," *Experimental Thermal and Fluid Science*, vol. 44, pp. 209-218, 2013. [CrossRef] [Google Scholar] [Publisher Link]

[2] Haowei Hu et al., "Effects of System Pressure on Nucleate Boiling: Insights from Molecular Dynamics," *Journal of Molecular Liquids*, vol. 402, 2024. [CrossRef] [Google Scholar] [Publisher Link]

[3] Peng Feng et al., "Experimental Investigation on Transition Boiling During Reflooding in a Narrow Rectangular Channel with High Wall Temperature," *Progress in Nuclear Energy*, vol. 170, pp. 1-29, 2024. [CrossRef] [Google Scholar] [Publisher Link]

[4] J.B. Schmidt et al., "Modelling of Drop and Spray Impact in the Transitional Boiling Regime," *International Journal of Heat and Mass Transfer*, vol. 217, pp. 1-27, 2023. [CrossRef] [Google Scholar] [Publisher Link]

[5] Xiaojing Ma et al., "Low Thermal Conductivity Substrate Accelerates Droplet Evaporation in Transition Boiling Regime: An Abnormal Leidenfrost Phenomenon," *Applied Thermal Engineering*, vol. 221, 2023. [CrossRef] [Google Scholar] [Publisher Link]

[6] Ji Li et al., "High Heat Flux Dissipation of Membrane-Venting Heat Sink with Thin Film Boiling," *International Journal of Heat and Mass Transfer*, vol. 221, 2024. [CrossRef] [Google Scholar] [Publisher Link]

[7] Pengkun Li et al., "Heat Transfer Incipience of Capillary-Driven Liquid Film Boiling," *Materials Today Physics*, vol. 38, 2023. [CrossRef] [Google Scholar] [Publisher Link]

[8] Wang Qi et al., "Numerical Analysis on Transition Sequence and Heat Transfer Capacity of Film Boiling with a Uniform Electric Field," *Physics of Fluids*, vol. 35, no. 5, pp. 1-24, 2023. [CrossRef] [Google Scholar] [Publisher Link]

[9] Jiayu Du et al., "Analytical Consideration for the Maximum Spreading Factor of Liquid Droplet Impact on a Smooth Solid Surface," *Langmuir*, vol. 37, no. 24, pp. 7582-7590, 2021. [CrossRef] [Google Scholar] [Publisher Link]

[10] Yi-Bo Wang et al., "Universal Model for the Maximum Spreading Factor of Impacting Nanodroplets: from Hydrophilic to Hydrophobic Surfaces," *Langmuir*, vol. 36, no. 31, pp. 9306-9316, 2020. [CrossRef] [Google Scholar] [Publisher Link]

[11] Denis Richard, Christophe Clanet, and David Quéré, "Contact Time of a Bouncing Drop," *Nature*, vol. 417, no. 6891, 2002. [CrossRef] [Google Scholar] [Publisher Link]

[12] Fang-Fang Xie et al., "Contact Time of a Bouncing Nanodroplet," *The Journal of Physical Chemistry Letters*, vol. 11, no. 8, pp. 2818-2823, 2020. [CrossRef] [Google Scholar] [Publisher Link]

[13] Jorge Duarte Benther et al., "Heat Transfer During Multiple Droplet Impingement and Spray Cooling: Review and Prospects for Enhanced Surfaces," *International Journal of Heat and Mass Transfer*, vol. 178, pp. 1-36, 2021. [CrossRef] [Google Scholar] [Publisher Link]

[14] Tianshi Zhang et al., "Advanced Study of Spray Cooling: from Theories to Applications," *Energies*, vol. 15, no. 23, pp. 1-40, 2022. [CrossRef] [Google Scholar] [Publisher Link]

[15] Dagnija Blumberga et al., "Innovative Scrubber Technology Model for Domestic Boiler Application," *International Journal of Energy and Environmental Engineering*, vol. 12, no. 1, pp. 11-21, 2021. [CrossRef] [Google Scholar] [Publisher Link]

[16] T.R. Valiullin et al., "An Experimental Investigation into Ignition and Combustion of Groups of Slurry Fuel Droplets Containing High Concentrations of Water," *Fuel Processing Technology*, vol. 210, 2020. [CrossRef] [Google Scholar] [Publisher Link]

[17] Detlef Lohse, "Fundamental Fluid Dynamics Challenges in Inkjet Printing," *Annual Review of Fluid Mechanics*, vol. 54, no. 1, pp. 349-382, 2022. [CrossRef] [Google Scholar] [Publisher Link]

[18] Jida Huang et al., "Unsupervised Learning for the Droplet Evolution Prediction and Process Dynamics Understanding in Inkjet Printing," *Additive Manufacturing*, vol. 35, pp. 1-14, 2020. [CrossRef] [Google Scholar] [Publisher Link]

[19] Zilong Zheng et al., "Preparation of Protective Coatings for the Leading Edge of Wind Turbine Blades and Investigation of their Water Droplet Erosion Behavior," *Wear*, vol. 558-559, 2024. [CrossRef] [Google Scholar] [Publisher Link]

[20] Zhe Li et al., "Adjusting Droplet Adhesion of Superhydrophobic Coating Via Surface Embedding of Microparticles with Mixed Shapes," *Chemical Engineering Journal*, vol. 492, 2024. [CrossRef] [Google Scholar] [Publisher Link]

[21] Haixiang Zhang et al., "Effect of Wettability on Droplet Impact: Spreading and Splashing," *Experimental Thermal and Fluid Science*, vol. 124, 2021. [CrossRef] [Google Scholar] [Publisher Link]

[22] Xiaonuo Huang, Leping Zhou, and Xiaoze Du, "Critical Contact Angle for Triggering Dynamic Leidenfrost Phenomenon at Different Surface Wettability: A Molecular Dynamics Study," *Journal of Molecular Liquids*, vol. 382, 2023. [CrossRef] [Google Scholar] [Publisher Link]

[23] Hsiang Yu Tsai et al., "Fast Spreading of Liquid on Leidenfrost Vapor Layer Surface," *Colloids and Surfaces A: Physicochemical and Engineering Aspects*, vol. 677, 2023. [CrossRef] [Google Scholar] [Publisher Link]

[24] Chang Cai et al., "Alcohol-Induced Elevation in the Dynamic Leidenfrost Point Temperature for Water Droplet Impact," *International Journal of Heat and Mass Transfer*, vol. 215, 2023. [CrossRef] [Google Scholar] [Publisher Link]

[25] Boris Kichatov et al., "Evaporation of Ferrofluid Drop in Magnetic Field in Leidenfrost Mode," *Journal of Magnetism and Magnetic Materials*, vol. 588, 2023. [CrossRef] [Google Scholar] [Publisher Link]

[26] Teguh Wibowo et al., "The Effect of Ethylene Glycol Concentration on the Interfacial Dynamics of the Successive Droplets Impacting onto a Horizontal Hot Solid Surface," *International Journal of Thermal Sciences*, vol. 159, 2021. [CrossRef] [Google Scholar] [Publisher Link]

[27] Ana Sofia Moita, and António Luís N. Moreira, "The Deformation of Single Droplets Impacting onto a Flat Surface," *SAE Transactions*, vol. 111, pp. 1477-1489, 2002. [Google Scholar] [Publisher Link]